The PPARβ/δ Activator GW501516 Prevents the Down-Regulation of AMPK Caused by a High-Fat Diet in Liver and Amplifies the PGC-1α-Lipin 1-PPARα Pathway Leading to Increased Fatty Acid Oxidation

Emma Barroso, Ricardo Rodríguez-Calvo, Lucía Serrano-Marco, Alma M. Astudillo, Jesús Balsinde, Xavier Palomer, and Manuel Vázquez-Carrera

Pharmacology Unit (E.B., R.R.-C., L.S.-M., X.P., M.V.-C.), Department of Pharmacology and Therapeutic Chemistry, and Institut de Biomedicina de la University of Barcelona, Faculty of Pharmacy, University of Barcelona, and Centro de Investigación Biomédica en Red de Diabetes y Enfermedades Metabólicas Asociadas-Instituto de Salud Carlos III (E.B., R.R.-C., L.S.-M., A.M.A., J.B., X.P., M.V.-C.), 08028 Barcelona, Spain; and Instituto de Biología y Genética Molecular (A.M.A., J.B.), Consejo Superior de Investigaciones Científicas, 47005 Valladolid, Spain

Metabolic syndrome-associated dyslipidemia is mainly initiated by hepatic overproduction of the plasma lipoproteins carrying triglycerides. Here we examined the effects of the peroxisome proliferator-activated receptors (PPAR)-β/δ activator GW501516 on high-fat diet (HFD)-induced hypertriglyceridemia and hepatic fatty acid oxidation. Exposure to the HFD caused hypertriglyceridemia that was accompanied by reduced hepatic mRNA levels of PPAR-γ coactivator 1 (PGC-1)-α and lipin 1, and these effects were prevented by GW501516 treatment. GW501516 treatment also increased nuclear lipin 1 protein levels, leading to amplification in the PGC-1α-PPARα signaling system, as demonstrated by the increase in PPARα levels and PPARα-DNA binding activity and the increased expression of PPARα-target genes involved in fatty acid oxidation. These effects of GW501516 were accompanied by an increase in plasma β-hydroxybutyrate levels, demonstrating enhanced hepatic fatty acid oxidation. Moreover, GW501516 increased the levels of the hepatic endogenous ligand for PPARα, 16:0/18:1-phosphatidilcholine and markedly enhanced the expression of the hepatic *Vldl receptor*. Interestingly, GW501516 prevented the reduction in AMP-activated protein kinase (AMPK) phosphorylation and the increase in phosphorylated levels of ERK1/2 caused by HFD. In addition, our data indicate that the activation of AMPK after GW501516 treatment in mice fed HFD might be the result of an increase in the AMP to ATP ratio in hepatocytes. These findings indicate that the hypotriglyceridemic effect of GW501516 in HFD-fed mice is accompanied by an increase in phospho-AMPK levels and the amplification of the PGC-1α-lipin 1-PPARα pathway. **(*Endocrinology* 152: 1848–1859, 2011)**

Excess caloric intake and nutrient availability have increased the incidence of obesity and insulin resistance, which are the main factors responsible for the development of metabolic syndrome. This condition is characterized by dyslipidemia, which is a major risk factor for cardiovascular disease, and predisposes to early atherosclerosis and cardiovascular morbidity (1). Dyslipidemia in metabolic syndrome is characterized by high levels of plasma triglycerides, low levels of high-density lipoprotein cholesterol, and the appearance of small, dense, low-density lipoproteins and excessive postprandial lipemia (2). It is now recognized that the dyslipidemia associated with

ISSN Print 0013-7227 ISSN Online 1945-7170
Printed in U.S.A.

doi: 10.1210/en.2010-1468 Received December 22, 2010. Accepted February 7, 2011.
First Published Online March 1, 2011

For editorial see page 1742

Abbreviations: AMPK, AMP-activated protein kinase; Aprt, adenosyl phosphoribosyl transferase; AUC, area under the curve; Cept1, cholineethanolamine phosphotransferase-1; CPT1a, carnitine palmitoyltransferase-1a; Cte, cytosolic thioesterase; FAS, fatty acid synthase; HFD, high-fat diet; 1-PC, 1-palmitoyl-2-oleyl-phosphatidilcholine; PGC, PPAR-γ coactivator 1; PP2A, protein phosphatase 2A; PPAR, peroxisome proliferator-activated receptor; PPRE, peroxisome proliferator response element; SIRT1, silent information regulator T1; VLDL, very low-density lipoprotein; Vldl-r, Vldl receptor.

the metabolic syndrome is mainly initiated by the hepatic overproduction of the plasma lipoproteins carrying triglycerides, the very low-density lipoproteins (VLDL), which induce a sequence of lipoprotein changes leading to atherogenic lipid abnormalities in metabolic syndrome (3). It is thus important to find new pharmacological treatments to reduce plasma triglyceride levels and thus prevent the development of atherogenic dyslipidemia in metabolic syndrome.

Among the new pharmacological treatments to prevent the increase in triglyceride levels, peroxisome proliferator-activated receptors (PPAR)-β/δ activators have attracted widespread attention. PPARs are members of the nuclear receptor superfamily of ligand-activated transcription factors that regulate the expression of genes involved in many important biological processes (4). The PPAR family consists of three members, PPARα (NR1C1 according to the unified nomenclature system for the nuclear receptor superfamily), PPARβ/δ (NR1C2), and PPARγ (NR1C3) (5). PPARα was the first to be identified and was demonstrated to be the molecular target of the fibrate hypolipidemic class of drugs. This PPAR isotype is expressed primarily in tissues that have a high level of fatty acid catabolism such as liver, brown fat, kidney, heart, and skeletal muscle (6). PPARγ has a restricted pattern of expression, mainly in white and brown adipose tissues and colon, and it is also expressed in macrophages, whereas other tissues such as skeletal muscle and heart contain limited amounts. PPARβ/δ is expressed ubiquitously, including metabolically active tissues such as liver, muscle, and fat, and its role in the metabolic syndrome has been elucidated in the last years (7–9).

Among other effects, treatment with the high-affinity PPARβ/δ ligand GW501516 has been shown to decrease triglycerides (10). In PPARβ/δ-null mice, the hypotriglyceridemic effect of PPARβ/δ has been associated with its effect on hepatic VLDL production and clearance (11), but the contribution of additional mechanisms has not been explored. Interestingly, the main factor influencing hepatic triglyceride secretion is fatty acid availability (12). In liver, fatty acids are either incorporated into triglycerides or oxidized by mitochondrial β-oxidation. An increase in fatty acid oxidation in liver would thus reduce the availability of fatty acids and subsequent hepatic triglyceride secretion. However, it is unknown whether the hypotriglyceridemic effect observed after PPARβ/δ activation involves increased hepatic fatty acid oxidation and the mechanisms involved. The rate-limiting step for mitochondrial β-oxidation is the transport of fatty acid into mitochondria by liver carnitine palmitoyltransferase-1 (CPT1a). This fatty acid transporter is under the control of both PPARs and AMP-activated protein kinase (AMPK), which detects low ATP levels and in turn increases oxidative metabolism (13) by reducing the levels of malonyl-CoA. Interestingly, PPARβ/δ activation can increase the activity of AMPK, and the increase in fatty acid oxidation in human skeletal muscle cells after GW501516 treatment is dependent on both PPARβ/δ and AMPK (14).

A novel protein, lipin 1, determines whether fatty acids are incorporated into triglycerides or undergo mitochondrial β-oxidation. The expression and compartmentalization of lipin 1 controls the secretion of hepatic triglycerides (15). Thus, in the cytoplasm, lipin 1 promotes triglyceride accumulation and phospholipid synthesis by functioning as an Mg^{2+}-dependent phosphatidate phosphatase (phosphatidic acid phosphatase-1). In contrast, in the nucleus lipin 1 acts as a transcriptional coactivator linked to fatty acid oxidation by regulating the induction of PPAR-γ coactivator 1 (PGC)-1α-PPARα-target genes (16). Lipin 1 induces PPARα gene expression and forms a complex with PPARα and PGC-1α leading to the induction of genes involved in fatty acid oxidation, including *Cpt1a* and *Mcad* (medium chain acyl-coA dehydrogenase) (16).

Here we examined the effects of the PPARβ/δ activator GW501516 on the hypertriglyceridemia induced by a high-fat diet (HFD) and on the hepatic fatty acid oxidation pathway. Exposure to HFD caused hypertriglyceridemia accompanied by reduced hepatic phospho-AMPK levels and increased activity of ERK1/2. Interestingly, drug treatment reduced hypertriglyceridemia, restored hepatic phosphorylated levels of AMPK and ERK1/2, and induced liver fatty acid oxidation through a mechanism involving increased activation of the lipin 1/PGC-1α-PPARα signaling system. The findings of this study indicate a new mechanism of action by which PPARβ/δ may contribute to the reversal of hypertriglyceridemia caused by HFD and point to hepatic AMPK, PGC-1α, and lipin 1 as pharmacological targets to prevent this dyslipidemia.

Materials and Methods

Materials

GW501516 was provided by Alexis Biochemicals (Lausen, Switzerland). [γ-^{32}P]dATP (3000 Ci/mmol) was purchased from Amersham Biosciences (Pisacataway, NJ). All other chemicals were from Sigma-Aldrich (St. Louis, MO).

Animals

Mice aged 5 wk were maintained under standard conditions of illumination (12 h light, 12 h dark cycle) and temperature (21 ± 1 C). They were fed a standard diet (Harlan, Barcelona, Spain) for 5 d before the study began. The animals were then randomly distributed into three experimental groups (n = 12 each): those fed the standard diet; those fed a Western-type HFD (35% fat by weight, 58% kcal from fat; Harlan Ibérica S.A.,

Barcelona, Spain) plus one daily oral gavage of vehicle [0.5% (wt/vol) carboxymethylcellullose medium viscosity]; and those fed a HFD plus one daily oral dose of 3 mg/kg · d of the PPARβ/δ agonist GW501516 dissolved in the vehicle. Before the end of the treatments, a glucose tolerance test was performed on mice fasted for 4 h. Animals received 2 g/kg body weight of glucose by ip injection, and blood was collected from the tail vein after 0, 20, 40, and 90 min. The body weight of the mice and the food intake were checked regularly during the treatment period. After 3 wk of treatment, mice were killed under isoflurane anesthesia. After collecting blood, serum samples were analyzed for triglycerides, glucose (Bayer Iberia, Sant Joan Despí, Spain), cholesterol, free fatty acids (Wako, Neuss, Germany), insulin (Amersham), adiponectin, and leptin (Linco, St. Charles, MO). The liver samples were frozen in liquid nitrogen and then stored at −80 C. These experiments conformed to the Guide for the Care and Use of Laboratory Animals published by the U.S. National Institutes of Health (NIH publication no. 85-23, revised 1996). All procedures were approved by the University of Barcelona Bioethics Committee, as stated in Law 5/21 July 1995 passed by the Generalitat de Catalunya (Autonomous Government of Catalonia).

Measurements of mRNA

Levels of mRNA were assessed by the RT-PCR as previously described (17). The sequences of the sense and antisense primers used for amplification were: *lipin 1*, 5′-CTGCAGACAGGTTGACGCCAA-3′ and 5′-TCTGGTGGATGAGCAGTCCCC-3′; *Pgc-1α*, 5′-CCCGTGGATGAAGACGGATTG-3′ and 5′-GTGGGTGTGGTTTGCTGCATG-3′; *Pparα*, 5′-GGCTCGGAGGGCTCTGTCATC-3′ and 5′-ACATGCACTGGCAGCAGTGGA-3′; *Cpt1a*, 5′-TATGTGAGGATGCTGCTT-3′ and 5′-CTCGGAGAGCTAAGCTTG-3′, *Mcad*, 5′-TGGAAAGCGGCTCACAAGCAG-3′ and 5′-CACCGCAGCTTTCCGGAATGT-3′; cytosolic thioesterase (*Cte*) 5′-CAGCCACCCCGAGGTAAAAGG-3′ and 5′-CCTTGAGGCCATCCTTGGTCA-3′; cholineethanolamine phosphotransferase-1 (*Cept1*) 5′-GCTAGGTGAGCCGCTCAGTGC-3′ and 5′-ATGGTGCCTCCTCCGTGACTG-3′; Vldl receptor (*Vldl-r*) 5′-GTTCAAGTGCAGAAGCGGGGA-3′ and 5′-CCGGGTTTTGGCATTCATCAA-3′; and adenosyl phosphoribosyl transferase (*Aprt*), 5′-AGCTTCCCGGACTTCCCCATC-3′ and 5′-GACCACTTTCTGCCCCGGTTC-3′. Amplification of each gene yielded a single band of the expected size (*lipin 1*: 225 bp; *Pgc-1α*: 228 bp; *Pparα*: 654 bp; *Cpt-1a*: 629 bp; *Mcad*: 216 bp; *Cte*: 244 bp; *Cept1*: 233 bp; *Vldl-r*: 227 bp; and *Aprt*: 329 bp). Preliminary experiments were carried out with various amounts of cDNA to determine nonsaturating conditions of PCR amplification for all the genes studied. Therefore, under these conditions, relative quantification of mRNA was assessed by the RT-PCR method used in this study (18). Radioactive bands were quantified by videodensitometric scanning (Vilber Lourmat Imaging, Marne-la-Vallée, France). The results for the expression of specific mRNAs are presented relative to the expression of the control gene (*Aprt*).

Isolation of nuclear extracts. Nuclear extracts were isolated as previously described (17).

Electrophoretic mobility shift assay

EMSA was performed using double-stranded oligonucleotides for the consensus binding site of PPAR [peroxisome proliferator response element (PPRE) probe; 5′-CAAAACTAGGTCAAAGGTCA-3′; Santa Cruz Biotechnology, Santa Cruz, CA] as previously described (19–21).

Immunoblotting

To obtain total protein, livers were homogenized in cold lysis buffer [5 mM Tris-HCl (pH 7.4), 1 mM EDTA, 0.1 mM phenylmethylsulfonyl fluoride, 1 mM sodium orthovanadate, 5.4 μg/ml aprotinin]. The homogenate was centrifuged at 16,700 × *g* for 30 min at 4 C. Protein concentration was measured by the Bradford method. Protein extracts were resolved by SDS-PAGE on 10% separation gels and transferred to Immobilon polyvinylidene diflouride membranes (Millipore, Bedford, MA). Western blot analysis was performed using antibodies against total AMPK, phospho-Thr^{172}-AMPK, total ERK1/2, phospho-ERK1/2, the catalytic subunit of protein phosphatase 2A (PP2A) (52F8) (Cell Signaling, Danvers, MA), lipin 1, PPARα, liver kinase B1, lamin B (Santa Cruz Biotechnologies), PGC-1α (Chemicon, Billerica, MA), and β-actin (Sigma). Detection was achieved using the EZ-ECL chemiluminescence kit (Amersham). Size of detected proteins was estimated using protein molecular-mass standards (Invitrogen, Barcelona, Spain).

Coimmunoprecipitation studies

Cell nuclear extracts were brought to a final volume of 250 μl with buffer containing 10 mM PBS, 50 mM KCl, 0.05 mM EDTA, 2.5 mM $MgCl_2$, 8.5% glycerol, 1 mM dithiothreitol, 0.1% Triton X-100, BSA 2%, and 1 mg/ml nonfat milk for 18 h at 4 C and incubated with 4 μg of antibody. Immunocomplex was captured by incubating the samples with 50 μl protein A-agarose suspension for 6 h at 4 C. Agarose beads were collected by centrifugation and washed. After microcentrifugation, the pellet was resuspended with SDS-PAGE sample buffer and boiled for 5 min at 100 C. The resulting supernatant was then subjected to electrophoresis on 10% SDS-PAGE and immunoblot analysis.

Determination of ceramide levels

The content of ceramides in liver was determined by the diacylglycerol kinase method as previously described (22).

Analysis of 1-palmitoyl-2-oleyl-phosphatidilcholine (16:0/18:1-PC)

Total lipids of liver homogenates were extracted according to Bligh and Dyer (23), evaporated, and redissolved in methanol-water (9:1). Total lipid separation, identification, and quantification was carried out by liquid chromatography/mass spectrometry using a Hitachi LaChrom Elite L-2130 binary pump and a Hitachi autosampler L-2200 (Merck, Darmstadt, Germany) coupled to a Bruker esquire6000 ion-trap mass spectrometer (24, 25). The effluent was split, entering 0.2 ml/min to the electrospray interface of the mass spectrometer. The nebulizer was set to 30 ψ, the dry gas to 8 l/min, and the dry temperature to 350 C. The column used was a Supelcosil LC-18 of 5 μm particle size, 250 × 2.1 mm (Sigma-Aldrich) protected with a Supelguard LC-18 20- × 2.1-mm guard cartridge column (Sigma-Aldrich). The mobile phase used was a gradient of solvent A [methanol/water/hexane/ammonium hydroxide, 87.5:10.5:1.5:0.5 (vol/vol/vol/vol], solvent B [(methanol/hexane/ammonium hydroxide, 87.5:12:0.5 vol/vol/vol], and solvent C [methanol/water, 9:1 (vol/vol)]. The gradient started at 100% A, decreased linearly to 50% A (50% B) in 17.5 min, and to 0% A (100% B)

in 12.5 min, mantained at 100% B for 5 min, and then changed to 100% C in 3 min, maintained 9 min, and changed to 100% B in 3 min. The flow rate was 0.5 ml/min and the injection volume was 80 μl. Data acquisition was carried out in full scan and positive mode, detecting PC species as $[M^+H]^+$ ions with the capillary current set at −4000 V. The PC (16:0/18:1) species were characterized by tandem mass spectrometry in multiple reaction monitoring and negative mode, with a postcolumn addition of acetic acid for $[M + CH_3CO_2]$-adduct formation (100 μl/h). 1,2-Dinonadecanoyl-sn-glycero-3-phosphocoline (m/z = 818.6) was used as internal standard and also in a calibration curve for quantitation.

HPLC measurement of ATP, ADP, and AMP

Adenine nucleotides were separated by HPLC using an X-Bridge column with a 3.5-μm outer diameter (100 × 4.6 cm). Elution was done with 0.1 mM potassium dihydrogen phosphate (pH 6), containing 4 mM tetrabutylammonium hydrogen sulfate and 15% (vol/vol) methanol. The conditions were as follows: 20 μl sample injection, column at room temperature, flow rate of 0.6 ml/min^{-1} and UV monitoring at 260 nm.

Statistical analyses

Results are expressed as means ± SD. Significant differences were established by one-way ANOVA using the GraphPad Instat program (GraphPad Software version 2.03; GraphPad Softwware Inc., San Diego, CA). When significant variations were found, the Tukey-Kramer multiple comparisons test was applied. Differences were considered significant at $P < 0.05$.

Results

Effects of GW501516 treatment on plasma lipid levels, liver triglyceride content, and glucose tolerance test in mice fed the HFD

Most of the studies performed using PPARβ/δ agonists were based on long-term drug treatment, leading to a significant reduction in weight loss and fat mass (26, 27), which affect both lipid metabolism and insulin sensitivity. To prevent the interference of weight loss in the parameters analyzed, mice were treated with the PPARβ/δ agonist for 3 wk. After this period, mice receiving the HFD or the HFD plus the drug showed no significant differences in body weight compared with control mice (control: 30.4 ± 2.8 g; HFD: 30.0 ± 2.5 g; and HFD+GW501516: 31.4 ± 2.7 g), and the amount of food consumed was similar in all three groups (data not shown). In addition, mice fed the HFD or HFD plus GW501516 showed no significant changes in the levels of plasma total cholesterol, glucose, insulin, adiponectin, leptin, or nonesterified fatty acids compared with controls (data not shown). In contrast, mice fed the HFD had enhanced plasma triglyceride levels compared with controls (55 ± 2.5 *vs.* 123 ± 29 mg/dl, 2.2-fold induction, $P < 0.05$), whereas this increase was abolished by GW501516 treatment (69 ± 16 mg/dl, $P <$ 0.01 *vs.* HFD-fed mice) (Fig. 1A). The HFD also enhanced the liver triglyceride content (4.5-fold induction, $P < 0.05$) (Fig. 1B). However, the drug treatment did not affect this parameter, which is in line with a previous study (9). When subjected to a glucose tolerance test, which evaluates the ability of the body to adjust glucose levels after an acute glucose injection, glucose levels of control mice peaked at 30 min and returned to the basal level (Fig. 1C). As expected, mice fed with the HFD were glucose intolerant, as demonstrated by the significant increase in the area under the curve (AUC). In contrast, mice fed with the HFD and treated with GW501516 showed an improved response to the glucose challenge, and the AUC of their glucose-tolerance test was similar to that of controls.

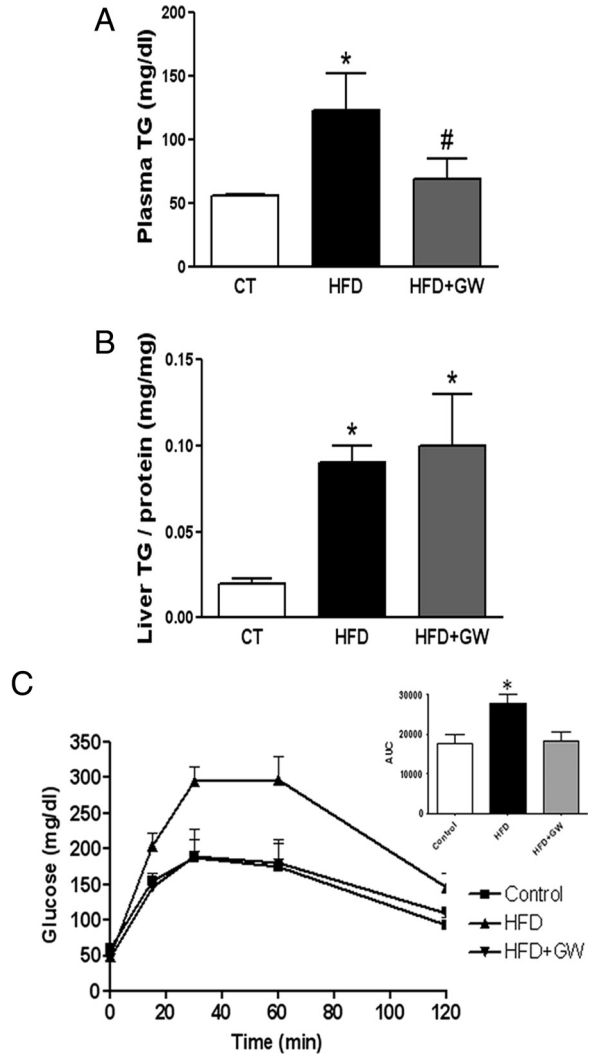

FIG. 1. GW501516 treatment prevents hypertriglyceridemia and glucose intolerance in mice fed a HFD. Mice were fed a standard chow or HFD with or without GW501516 (3 mg/kg · d). After 3 wk of treatment, blood samples and livers were obtained. A, Plasma triglyceride levels. B, Hepatic triglyceride content. C, Glucose tolerance test and AUC (*right panel*). Data are expressed as means ± SD (six mice per group). GW, GW501516. *, $P < 0.05$ *vs.* control mice; #, $P < 0.05$ *vs.* HFD-fed mice.

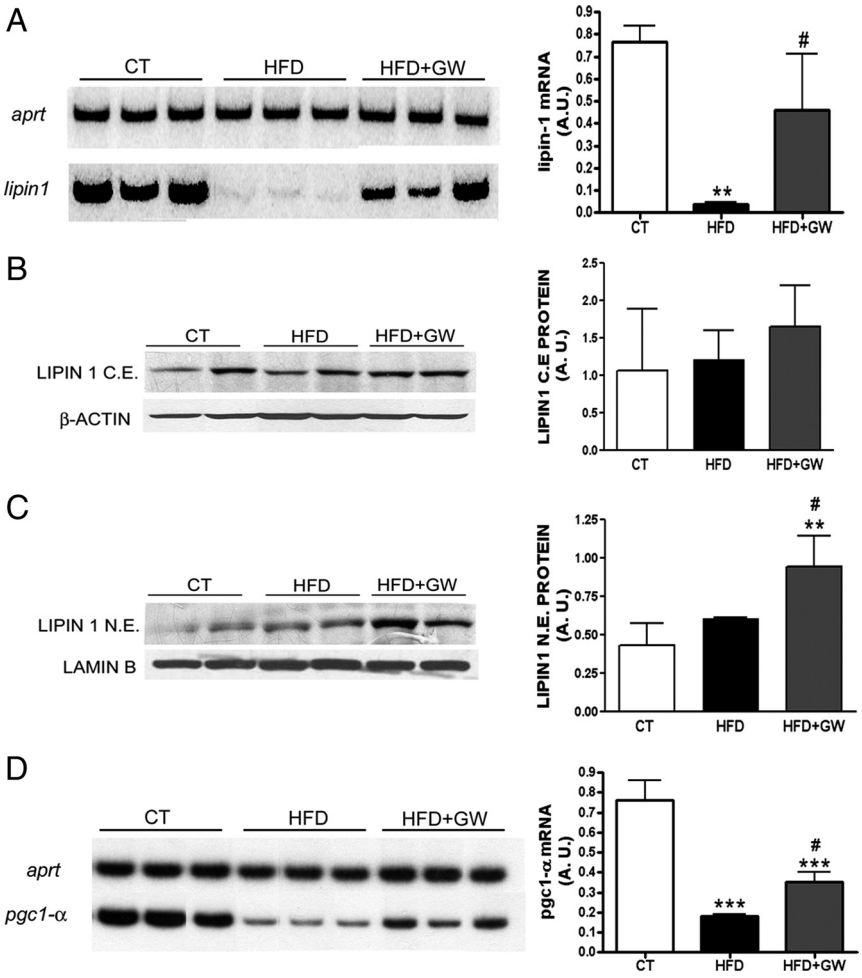

FIG. 2. GW501516 treatment increases nuclear lipin 1 in liver of mice fed a HFD. A, Effects of GW501516 on the mRNA levels of *Lipin 1*. Total RNA was isolated and analyzed by RT-PCR. A representative autoradiogram and the quantification normalized to the *Aprt* mRNA levels are shown. Data are expressed as means ± SD (five mice per group). Analysis of lipin 1 protein levels by immunoblotting of cytosolic (C.E.) (B) and nuclear (N.E.) (C) protein extracts from livers. To show equal loading of protein, the β-actin (total protein) or lamin B (nuclear protein) signal from the same blot is included. D, Effects of GW501516 on the mRNA levels of *Pgc-1α*; CT, control; GW, GW501516. **, $P < 0.01$, and ***, $P < 0.001$ *vs.* control mice; #, $P < 0.05$, ##, $P < 0.01$ *vs.* HFD-fed mice.

GW501516 treatment restores PGC-1α expression and increases nuclear lipin 1 in liver of mice fed the HFD

To gain further understanding of the effects of GW501516 on the fate of fatty acids, either incorporated into triglycerides or oxidized, we analyzed the levels of lipin 1, which has been reported to be under the control of AMPK (28). The HFD strongly reduced the hepatic mRNA levels of lipin 1 compared with mice fed a standard diet, and this reduction was prevented in mice treated with the PPARβ/δ activator (Fig. 2A). The cytosolic protein levels of lipin 1 were not significantly affected by the HFD or the drug treatment (Fig. 2B). In contrast, GW501516 increased the protein levels of lipin 1 in the nucleus (Fig. 2C), in which it acts as a transcriptional coactivator linked to fatty acid oxidation (16). Likewise, the expression of the transcriptional coactivator PGC-1α, involved in fatty acid oxidation, was markedly reduced by HFD in liver, and this reduction was prevented by GW501516 (Fig. 2C).

GW501516 treatment increases PPARα expression and activity and fatty acid oxidation in liver of mice fed the HFD

Because it has been reported that hepatic lipin 1 overexpression results in enhanced expression of *Pparα* gene and its target genes, such as *Cpt1a* and *Mcad* (16), we assessed whether the increase in nuclear lipin 1 protein levels caused by GW501516 treatment led to these changes. GW501516 increased the mRNA and the nuclear protein levels of PPARα (Fig. 3, A and B). In addition, given that it has been demonstrated that lipin 1 activates the transcription of PPARα in cooperation with PGC-1α (16), we evaluated the effect of drug treatment on PPARα DNA-binding activity by performing EMSA. The PPRE probe formed two main complexes (I and II) with hepatic nuclear proteins (Fig. 3C). The specificity of these two DNA-binding complexes was assessed in competition experiments by adding an excess of unlabeled PPRE oligonucleotide. PPARα DNA-binding activity was higher in mice fed HFD plus GW501516 than in control and HFD-fed mice. Addition of antibody against PPARα supershifted complex II, thereby indicating that this complex contained PPARα. In contrast, no supershift was observed with an antibody against PPARβ. In line with the increase in the expression of PPARα and its DNA-binding activity, GW501516 treatment increased the expression of the PPAR-target genes *Mcad*, *Cte*, and *Cpt1a* compared with control and HFD-fed mice (Fig. 3, D–F). Consistent with the increase in the expression of PPARα-target genes involved in hepatic fatty acid oxidation, levels of plasma β-hydroxybutyrate, a product of ketogenesis used as a marker of hepatic fatty acid oxidation, were significantly elevated in mice receiving the HFD plus GW501516 (Fig. 3G). Collectively, these findings indicate that GW501516, similarly to overexpression of *Lipin 1* (16), amplifies the

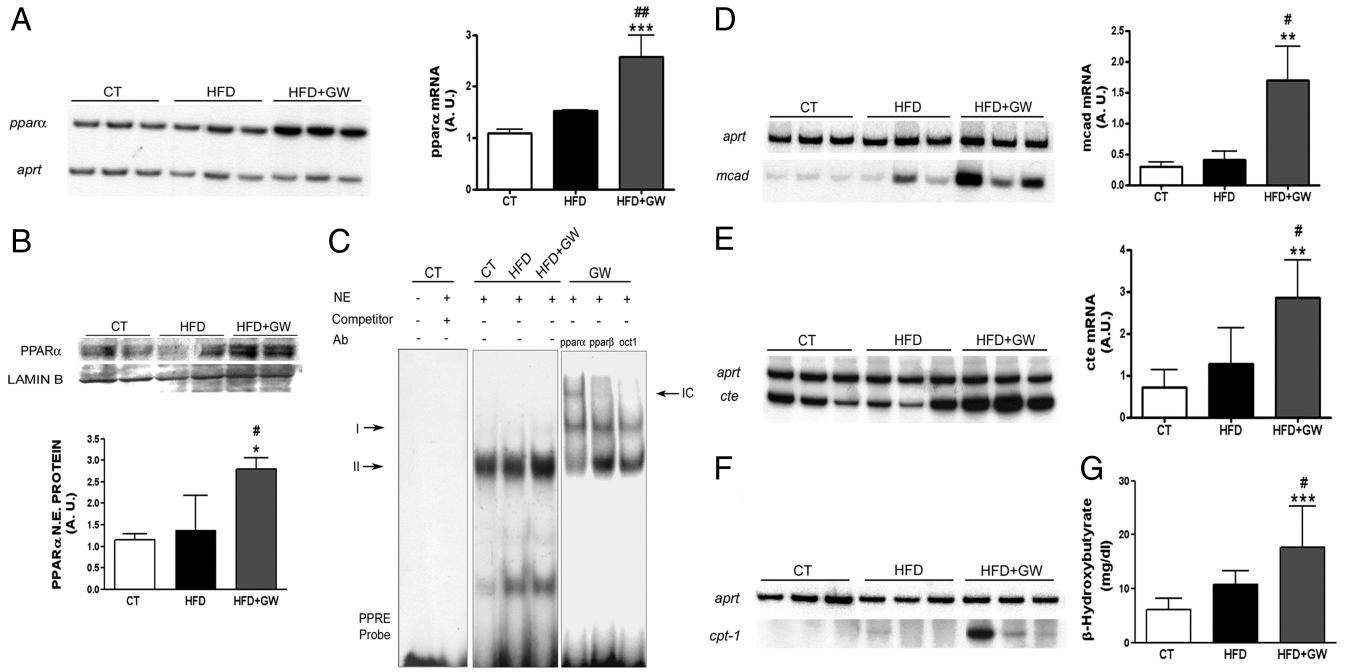

FIG. 3. GW501516 treatment increases PPARα expression and its DNA-binding activity and fatty acid oxidation in liver of mice fed HFD. A, mRNA levels of *Pparα* in the livers of mice fed a standard chow or HFD with or without GW501516. Total RNA was isolated and analyzed by RT-PCR. A representative autoradiogram and the quantification normalized to the *Aprt* mRNA levels are shown. B, Analysis of PPARα protein levels by immunoblotting of nuclear protein extracts from livers. To show equal loading of protein, the lamin B signal is included from the same blot. C, Autoradiograph of EMSA performed with a ^{32}P-labeled PPRE nucleotide and nuclear protein extract (NE). Two specific complexes (I and II), based on competition with a molar excess of unlabeled probe are shown. A supershift analysis was performed by incubating NE with an antibody directed against PPARα, PPARβ, and Oct-1. IC, Immunocomplex; CT, control; GW, GW501516. Effects of GW501516 on the mRNA levels of *Mcad* (D), *Cte* (E), and *Cpt-1a* (F). G, Plasma β-hydroxybutyrate levels in mice fed a standard chow or HFD with or without GW501516. Data are expressed as means ± SD (five mice per group). *, $P < 0.05$, **, $P < 0.01$ and ***, $P < 0.001$ *vs.* control mice; #, $P < 0.05$ *vs.* HFD-fed mice; ##, $P < 0.01$ *vs.* HFD-fed mice.

PPARα-PGC-1α pathway and thus increases hepatic fatty acid oxidation.

GW501516 treatment increases the levels of the hepatic endogenous PPARα ligand 16:0/18:1-PC in mice fed the HFD

The increase in the PPARα pathway after GW501516 treatment was higher than that expected on the basis of the increase in Lipin 1. This led us to speculate that additional mechanisms might contribute to the effects observed after GW501516 treatment. We focused on the possibility that GW501516 might increase the levels of an endogenous ligand of PPARα. An endogenous ligand for PPARα in liver has recently been reported, 16:0/18:1-PC (29). The synthesis of this ligand involves the enzymatic activity of CEPT1, and overexpression of *Cept1* in hepatoma cells increases the expression of PPARα-target genes, such as *Cpt1a* (29). First, we determined whether GW501516 affected the expression of *Cept1*. Both, HFD and HFD plus GW501516 increased *Cept1* expression, but the increase attributable to GW501516 was significantly higher than that caused by HFD alone (Fig. 4A). Interestingly, when we analyzed the levels of 16:0/18:1-PC, only those mice receiving the GW501516 showed increased levels of this PPARα endogenous ligand (Fig. 4B).

GW501516 treatment increases the mRNA levels of hepatic *Vldl-r* in mice fed the HFD

The increase in hepatic fatty acid oxidation after GW501516 treatment seemed to be inconsistent with the lack of effect of this drug on hepatic triglyceride content. Although this has been reported to be the result of the increase in glucose flux through the pentose phosphate pathway and enhanced fatty acid synthesis caused by GW501516 (9), we explored additional mechanisms by studying the effects of this drug on the *Vldl-r*, which may be a novel PPARβ/δ-target gene (30), and its expression may be increased by AMPK (31). This receptor is expressed abundantly in heart, skeletal muscle, and adipose tissue but only in trace amounts in the liver (32). In addition, *in vitro* studies have shown that the VLDL receptor binds and internalizes triglyceride-rich lipoproteins, including VLDL, in adipose tissue and skeletal muscle, thus reducing plasma triglyceride levels (33). In line with this, expression of the *Vldl-r* was high in skeletal muscle (Fig. 5A) and absent in liver (Fig. 5B) of control mice. Interestingly, GW501516 did not affect *Vldl-r* expression in skeletal muscle, although it increased it in liver (Fig. 5). These findings may contribute in explaining both the reduction in plasma triglycerides and the lack of reduction in the content of liver triglycerides after GW501516 treatment as a result of increased liver triglyceride uptake from the plasma.

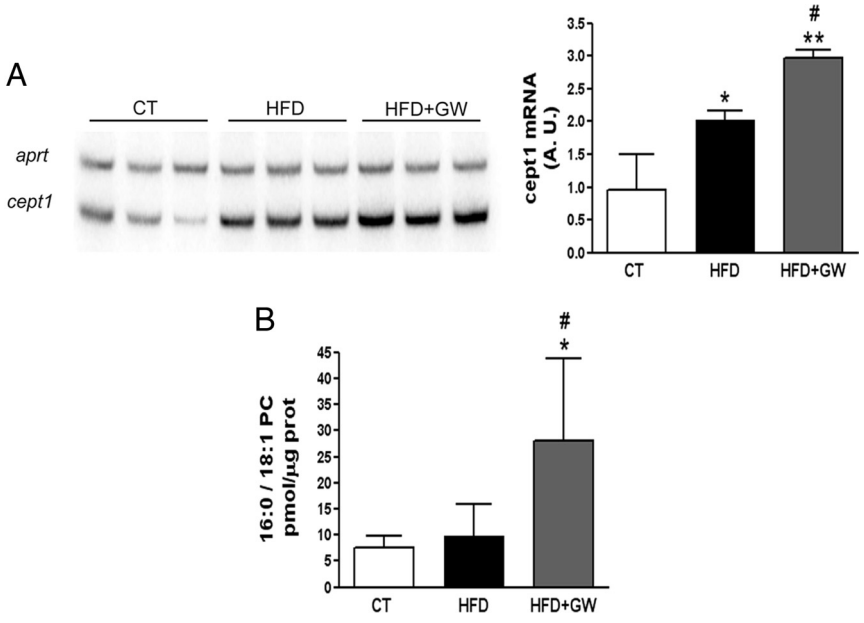

FIG. 4. GW501516 treatment increases the levels of the hepatic endogenous PPARα ligand 16:0/18:1-PC in mice fed HFD. A, mRNA levels of *Cept-1* in the livers of mice fed a standard chow or HFD with or without GW501516. Total RNA was isolated and analyzed by RT-PCR. A representative autoradiogram and the quantification normalized to the *Aprt* mRNA levels are shown. B, Quantification of 16:0/18:1-PC in nuclear extracts from livers of mice fed a standard chow or HFD with or without GW501516. Data are expressed as means ± SD (five mice per group). CT, Control; GW, GW501516. *, $P < 0.05$ and **, $P < 0.01$ *vs.* control mice; #, $P < 0.05$ *vs.* HFD-fed mice.

GW501516 treatment restores phospho-AMPK and increases AMP to ATP ratio in liver of mice fed the HFD

Given the prominent role of AMPK in liver fatty acid oxidation (13) and the fact that this kinase up-regulates the expression of *Lipin 1* (28), the *Vldl-r* (31) and *Pgc-1α* (34), we analyzed the hepatic levels of total and phosphorylated AMPK. In agreement with previous studies (35), HFD reduced phospho-AMPKα levels in liver (Fig. 6A). Interestingly, GW501516 treatment blunted this reduction. Because inhibitory cross talk between AMPK and ERK1/2 has been reported (36) and because AMPK inhibition increases ERK1/2 phosphorylation in liver (37), we examined the phosphorylation status of this kinase. The reduction in phospho-AMPKα observed in mice fed the HFD was accompanied by an increase in phospho-ERK1/2 levels, whereas this increase was attenuated by GW501516 treatment (Fig. 6B). Because the prevention of the reduction in phospho-AMPK levels after GW501516 treatment may be responsible for the increase in the lipin 1/PPARα-PGC-1α signaling system, we explored the potential mechanisms involved. The control of AMPK is complex and its phosphorylation status is regulated by both phosphatases and kinases (13). First, we evaluated whether the reduction in phospho-AMPK caused by the HFD was dependent on activation of PP2A activation via ceramide accumulation, as previously reported (38). When we analyzed the content of ceramide and the abundance of the PP2A catalytic subunit, we did not detect significant changes in the different groups of study, suggesting that this pathway was not involved in the changes observed (Fig. 7, A and B). AMPK is activated by upstream kinases: a Ca2+-dependent pathway mediated by Ca2+/calmodulin-dependent protein kinase kinase-β, the pathway mediated by TGFβ-activated kinase-1 and especially by the AMP-dependent pathway mediated by LKB1 (the tumor suppressor kinase) (13). Interestingly, LKB1 deacetylation is regulated by silent information regulator T1 (SIRT1) (39), influencing its ability to activate AMPK, and it has been recently reported that PPARβ/δ increases SIRT1 expression (40). Thus, we explored whether SIRT1 was involved in the changes observed after GW501516 treatment. The protein levels of SIRT1 were higher in the liver of both mice fed

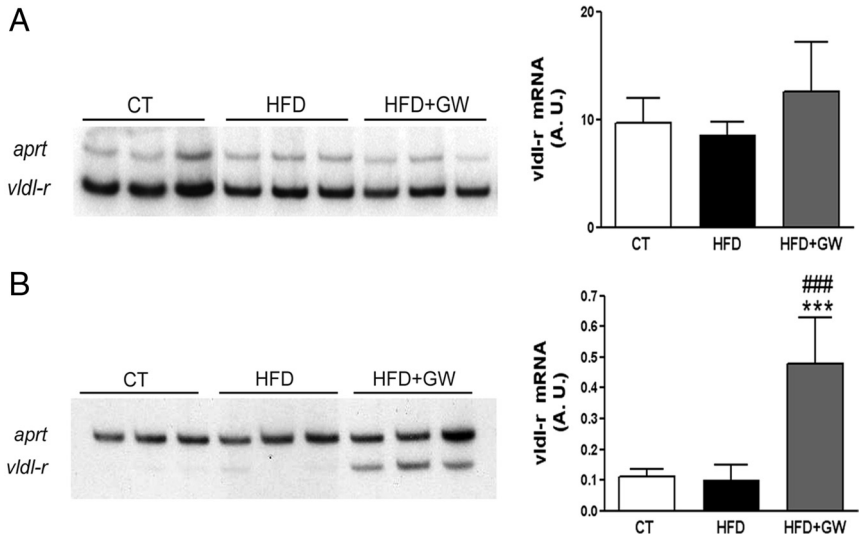

FIG. 5. GW501516 treatment increases the mRNA levels of hepatic VLDL receptor in mice fed HFD. *Vldl-r* mRNA levels in skeletal muscle (A) and liver (B) of mice fed a standard chow or HFD with or without GW501516. Total RNA was isolated and analyzed by RT-PCR. A representative autoradiogram and the quantification normalized to the *Aprt* mRNA levels are shown. Data are expressed as means ± SD (five mice per group). CT, Control; GW, GW501516. ***, $P < 0.001$ *vs.* control mice; ###, $P < 0.001$ *vs.* HFD-fed mice.

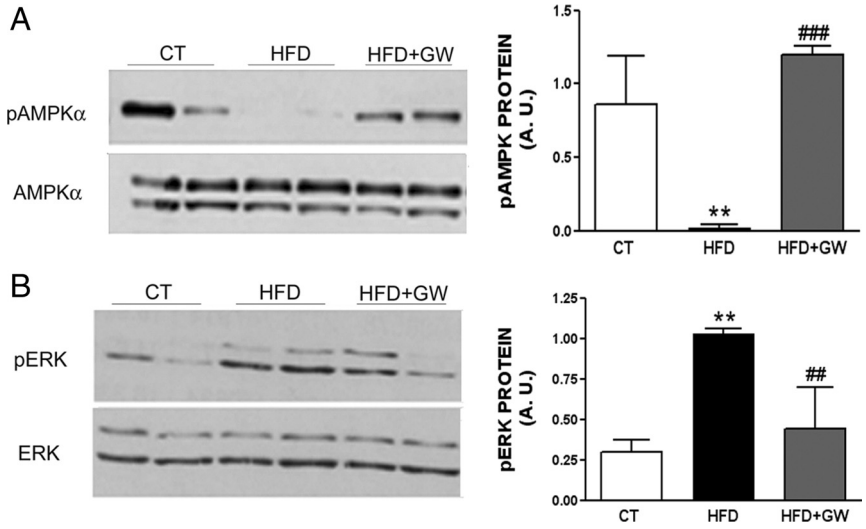

FIG. 6. GW501516 treatment prevents the reduction in phospho-AMPK and PGC-1α in liver of mice fed a HFD. Analysis of protein levels of phospho-AMPK (A) and phospho-ERK1/2 (B) in the livers of mice fed a standard chow or HFD with or without GW501516. Autoradiograph data are representative of three separate experiments. CT, Control; GW, GW501516. *, $P < 0.05$, **, $P < 0.01$, and ***, $P < 0.001$ *vs.* control mice; #, $P < 0.05$; ##, $P < 0.01$ *vs.* HFD-fed mice; ###, $P < 0.001$ *vs.* HFD-fed mice.

with HFD and mice fed with HFD plus GW501516 compared with control mice (Fig. 7C). However, when we examined the acetylation status of LKB1, we did not observe changes (Fig. 7D), suggesting that SIRT1 was not involved in AMPK regulation by GW501516. Finally, because AMPK is activated by an increase in the AMP to ATP ratio, we measured adenine nucleotide concentrations by HPLC in liver to determine the hepatic ATP to ADP and AMP to ATP ratios to further investigate the underlying mechanism of GW501516 on AMPK activation. GW501516 significantly increased the AMP to ATP ratio (Fig. 7E) and decreased the ATP to ADP ratio (Fig. 7F) compared with control and HFD-diet fed mice. Overall, these findings indicate that the increase in AMPK phosphorylation after GW501516 treatment was caused by a reduction in hepatocyte energy status.

Discussion

Excessive caloric intake can convert fatty acids into signaling molecules that, in liver, accelerate the production of glucose and lipoproteins, which contribute to the development of human diseases, such as obesity, insulin resistance, and metabolic syndrome. PPARβ/δ agonists are promising drugs for the treatment of these diseases. We followed a pharmacological approach to examine the role of PPARβ/δ in regulating fatty acid oxidation in liver of mice fed an HFD. Our findings demonstrate that treatment with the PPARβ/δ agonist GW501516 prevents the development of hypertriglyceridemia caused by the HFD. They also show that drug treatment prevents the reduction in hepatic phospho-AMPK levels induced by HFD and increases hepatic fatty acid oxidation by amplifying the activity of the lipin 1-PPARα-PGC-1α pathway.

Hepatocytes are exposed to dietary signals (from portal blood flow) and systemic signals (from the arterial blood supply). In contrast to other studies using long-term exposures to the HFD, mice were challenged with HFD for a short period of 3 wk to examine the seminal changes involved in the development of metabolic dysregulation caused by this diet. Mice exposed to HFD developed hypertriglyceridemia and glucose intolerance, but they did not show significant differences in plasma nonesterified fatty acids, leptin, or adiponectin, thus avoiding the interfering effects of these systemic adipocyte-derived signals on liver metabolism. Exposure to HFD also led to a reduction in hepatic phospho-AMPK levels that was prevented by GW501516. The maintenance of AMPK phosphorylation was accompanied by the recovery in the expression levels of *Lipin 1* and *Pgc-1α* and the increase in the mRNA levels of the *Vldl-r* (Fig. 8). Although we cannot rule out direct transcriptional activation of these gene by PPARβ/δ, because it has been suggested that *Lipin 1*, the *Vldl-r* (30), and *Pgc-1α* (41) might be PPARβ/δ-target genes, most effects of GW501516 may be the result of the increase in AMPK phosphorylation (14). In fact, it has been reported that this kinase up-regulates the expression of *Lipin 1* (28), the *Vldl-r* (31), and *Pgc-1α* (34).

The increase in AMPK phosphorylation after GW501516 treatment might involve several mechanisms. Because inhibitory cross talk between ERK1/2 and AMPK has been reported (36), the increase in phospho-AMPK levels could be the result of the inhibition by GW501516 of the phosphorylation of ERK1/2 induced by the HFD, which is in agreement with our previous study reporting that GW501516 prevents lipopolysaccharide-induced ERK1/2 phosphorylation in adipocytes (42). It is important to note that a previous study found that obesity leads to increased hepatic ERK1/2 activity and that caloric restriction blunts this increase and improves insulin sensitivity (43). In the present study, the improvement in glucose tolerance caused by GW501516 was also accompanied by the reduction in phospho-ERK1/2 levels. An additional mechanism could involve SIRT1 because it has recently been reported that pharmacological PPARβ/δ

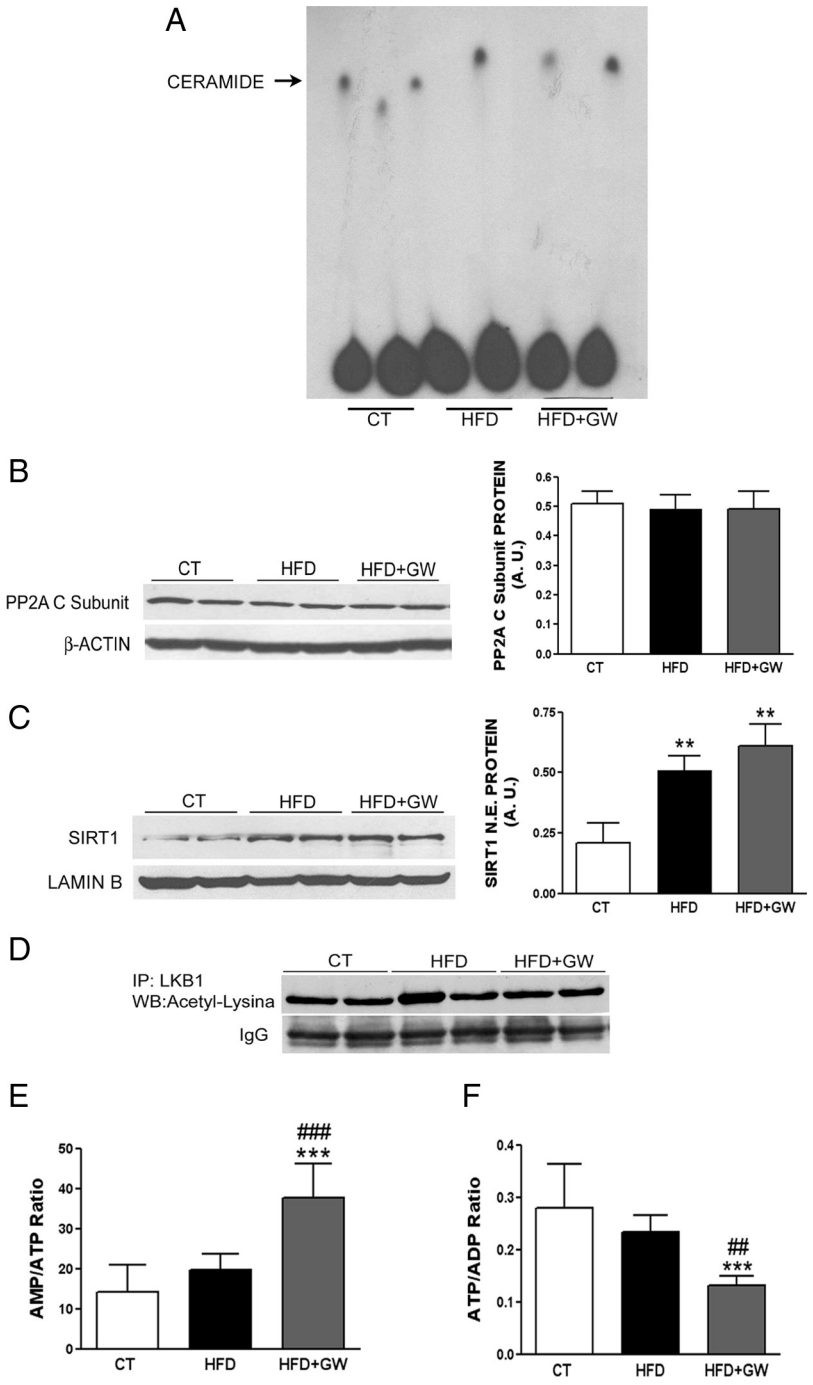

FIG. 7. GW501516 increases the AMP to ATP ratio in liver of mice treated with GW501516. A, Measurement of ceramide levels in the livers of mice fed a standard chow or HFD with or without GW501516. Lipid extracts from livers were prepared and assayed for ceramides as detailed in experimental procedures. Phosphorimage of phosphorylated ceramides, separated by thin-layer chromatography, is shown. Analysis of PP2AC (total protein) (B) and SIRT1 (nuclear extracts) (C) by immunoblotting is shown. The blot data are representative of four separate experiments. D, Acetylated levels of LKB1. Immunoprecipitation was performed with an antibody to LKB1 and immunoblotted with an acetyl-lysine antibody. The blot data are representative of four separate experiments. AMP to ATP (E) and ATP to ADP (F) ratios in the livers of mice fed a standard chow or HFD with or without GW501516 are shown. Results are means ± SD for data form six livers. CT, Control; GW, GW501516. **, $P < 0.01$ *vs*. control mice; ***, $P < 0.001$ *vs*. control mice; ##, $P < 0.01$, ###, $P < 0.001$ *vs*. HFD-fed mice.

activation increases the expression of SIRT1 (40), a deacetylase that regulates AMPK activity (44) through LKB1 acetylation (39) and might be essential to the regulatory loop involving PPARα, PGC-1α and lipin 1 (45). However, our findings make this possibility unlikely, given that the increase in SIRT1 levels induced by GW501516 did not modify the acetylation status of LKB1. Interestingly, here we show that GW501516 increases the AMP to ATP ratio in liver, indicating that, in line with a previous study in skeletal muscle cells (14), the underlying mechanism responsible for the increase in AMPK phosphorylation induced by this drug could be a modification of cellular energy status. Previous studies have suggested that the reduction in ATP levels caused by GW501516 can be the result of a specific inhibition of one or more complexes of the respiratory chain, an effect on the ATP synthase system, or to mitochondrial uncoupling (14). These potential changes would reduce the yield of ATP synthesis by the mitochondria, leading to AMPK activation.

In agreement with the reported regulation of PGC-1α (34, 46, 47) and lipin 1 (28) by AMPK, exposure to the HFD reduced both *Pgc-1α* and *Lipin 1* expression. The reduction in lipin 1 is likely to be the result of the decrease of PGC-1α because it has been reported that genetic reduction of hepatic PGC-1α decreases the expression of *Lipin 1* (48). In addition, it has been shown that physiological stimuli that increase mitochondrial fatty acid oxidation induce *Pgc-1α* gene expression, which in turn activates the expression of *Lipin 1* (16). Interestingly, it has been reported that up-regulation of lipin 1 in liver increases PPARα activity by two mechanisms: transcriptional activation of the *Pparα* gene and direct coactivation of PPARα in cooperation with PGC-1α (16). Thus, lipin 1 is considered to be an inducible booster that amplifies pathways downstream PGC-1α-PPARα, mainly mitochondrial fatty acid oxidation (16). In agreement with this, GW501516 treatment prevented the reduction in PGC-1α, increased the nuclear protein levels of lipin 1, and amplified the PGC-1α-PPARα pathway, as demonstrated by the increase in the

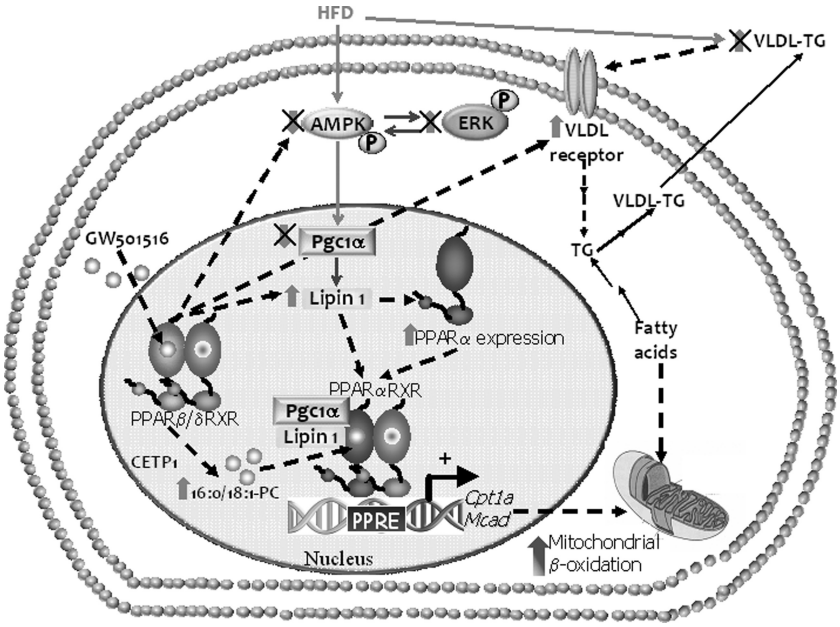

FIG. 8. A schematic of the potential effects of GW501516 (*dashed lines*) on liver metabolism is shown. Drug treatment with the PPARβ/δ agonist GW501516 prevents the reduction in phospho-AMPK levels and the subsequent increase in phospho-ERK1/2 levels caused by the HFD. In addition, GW501516 prevents the reduction in PGC-1α and increases lipin 1 protein levels in the nucleus leading to amplification of the PPARα-PGC-1α pathway, which subsequently induces hepatic fatty acid oxidation. This pathway is additionally increased by GW501516 through the enhanced synthesis of the hepatic PPARα endogenous ligand 16:0/18:1-PC. As a result of the increase in this pathway, the availability of fatty acids to be secreted as triglycerides might be compromised. The increase in the hepatic levels of the VLDL receptor can also contribute to reduce plasma triglyceride levels. TG, Triglyceride; P, phospho-protein.

transcriptional activation of *Pparα* and the increase in PPARα transcriptional activity (shown by the EMSA and enhanced PPARα-target gene expression). These effects subsequently enhanced hepatic fatty acid oxidation, as shown by the increase in β-hydroxybutyrate levels. The reduction in PGC-1α and lipin 1 levels caused by the HFD and their restoration after GW501516 treatment observed in this study may also contribute to the changes of plasma triglyceride levels because both proteins are involved in the control of hepatic triglyceride secretion and fatty acid oxidation (48–50). Overall, these data implicate PGC-1α and lipin 1 in the hypotriglyceridemic effect of PPARβ/δ and complement the findings of a previous study reporting that elevated plasma triglyceride levels in PPARβ/δ-null mouse were related to a combination of increased VLDL production and decreased plasma triglyceride clearance (11).

The data reported here also demonstrate that PPARβ/δ activation by GW501516 can amplify the PPARα pathway by an additional mechanism. Previous studies had demonstrated that hepatic fatty acid synthase (FAS) was necessary for the normal activation of PPARα target genes but did not identify the ligand involved in this process (51). Recently this endogenous PPARα ligand was identified as 16:0/18:1-PC (29). The synthesis of this ligand requires FAS activity, which yields palmitate (16:0), whereas 16:0/18:1-PC is generated through the enzymatic activity of CEPT1 (29). Subsequent binding of 16:0/18:1-PC to PPARα in the nucleus turns on PPARα-dependent genes and affects hepatic lipid metabolism. Interestingly, activation of PPARβ/δ by GW501516 induces FAS expression in liver as a result of increased glycolysis and the pentose phosphate shunt (9). Our findings confirm that GW501516 also increases *Cept1* expression and the levels of 16:0/18:1-PC, contributing to further amplification of the PPARα pathway.

The increase in fatty acid oxidation caused by GW501516 is apparently inconsistent with its lack of effects on hepatic triglyceride levels. Several reasons may account for this. First, similar to the effects of GW501516, which restores lipin 1 levels, hepatic *Lipin 1* overexpression leads to increased liver triglyceride content (16). This apparently conflicts with the effects of lipin 1 on fatty acid oxidation, but it has been explained by hepatic triglyceride sequestration secondary to diminished triglyceride secretion, increased fatty acid uptake, or the phosphatidic acid phosphatase activity of lipin 1 (16). Second, in this study we report an additional possibility, the increase caused by GW501516 in the expression of the *Vldl-r* in liver. The huge increase of this receptor observed in liver after GW501516 treatment might also reduce plasma triglyceride levels by increasing VLDL uptake by the liver. However, this can also lead to an increase in hepatic triglyceride content. Third, it has been reported that GW501516 improves hyperglycemia by increasing glucose flux through the pentose phosphate pathway and enhancing fatty acid synthesis in liver (9). In that study, GW501516 increased liver triglyceride content, but the authors reported that although this might raise concerns that long-term drug treatment might cause hepatic steatosis, they did not observe signs of fatty liver with treatment up to 6 months. In addition, long-term GW501516 treatment has been shown to reduce body weight and levels of circulating and liver triglycerides (26, 52).

In summary, our findings indicate that PPARβ/δ activation by GW501516 amplifies the PPARα-PGC-1α pathway through the restoration of AMPK activity, contributing to the hypotriglyceridemic effect of this drug.

Acknowledgments

We thank the University of Barcelona's Language Advisory Service for its help. Centro de Investigación Biomédica en Red de Diabetes y Enfermedades Metabólicas Asociadas is an initiative of Instituto de Salud Carlos III (Ministerio de Ciencia e Innovación). We also thank Ester Miralles for technical assistance with HPLC.

Address all correspondence and requests for reprints to: Manuel Vázquez-Carrera. Unitat de Farmacologia, Facultat de Farmàcia, Diagonal 643, E-08028 Barcelona. Spain. E-mail: mvazquezcarrera@ub.edu.

This work was partly supported by funds from the Spanish Ministerio de Ciencia e Innovación (SAF2009-06939 and BFU2010-18826) and the European Union European Regional Development Fund funds. R.R.-C. was supported by a grant from the Fundación Ramón Areces. L.S.-M. was supported by a Formación de Personal Investigador grant from the Spanish Ministerio de Ciencia e Innovación. A.M.A. was supported by a predoctoral fellowship from the Regional Government of Castilla y León (Spain).

Disclosure Summary: The authors have nothing to disclose.

References

1. **Bertoni AG, Wong ND, Shea S, Ma S, Liu K, Preethi S, Jacobs Jr DR, Wu C, Saad MF, Szklo M** 2007 Insulin resistance, metabolic syndrome, and subclinical atherosclerosis: the Multi-Ethnic Study of Atherosclerosis (MESA). Diabetes Care 30:2951–2956
2. **Grundy SM** 1998 Hypertriglyceridemia, atherogenic dyslipidemia, and the metabolic syndrome. Am J Cardiol 81:18B–25B
3. **Adiels M, Olofsson SO, Taskinen MR, Borén J** 2008 Overproduction of very low-density lipoproteins is the hallmark of the dyslipidemia in the metabolic syndrome. Arterioscler Thromb Vasc Biol 28:1225–1236
4. **Kersten S, Desvergne B, Wahli W** 2000 Roles of PPARs in health and disease. Nature 405:421–424
5. **Michalik L, Auwerx J, Berger JP, Chatterjee VK, Glass CK, Gonzalez FJ, Grimaldi PA, Kadowaki T, Lazar MA, O'Rahilly S, Palmer CN, Plutzky J, Reddy JK, Spiegelman BM, Staels B, Wahli W** 2006 International Union of Pharmacology. LXI. Peroxisome proliferator-activated receptors. Pharmacol Rev 58:726–741
6. **Braissant O, Foufelle F, Scotto C, Dauça M, Wahli W** 1996 Differential expression of peroxisome proliferator-activated receptors (PPARs): tissue distribution of PPAR-α, -β, and -γ in the adult rat. Endocrinology 137:354–366
7. **Barak Y, Liao D, He W, Ong ES, Nelson MC, Olefsky JM, Boland R, Evans RM** 2002 Effects of peroxisome proliferator-activated receptor δ on placentation, adiposity, and colorectal cancer. Proc Natl Acad Sci USA 99:303–308
8. **Peters JM, Lee SS, Li W, Ward JM, Gavrilova O, Everett C, Reitman ML, Hudson LD, Gonzalez FJ** 2000 Growth, adipose, brain, and skin alterations resulting from targeted disruption of the mouse peroxisome proliferator-activated receptor β(δ). Mol Cell Biol 20: 5119–5128
9. **Lee CH, Olson P, Hevener A, Mehl I, Chong LW, Olefsky JM, Gonzalez FJ, Ham J, Kang H, Peters JM, Evans RM** 2006 PPARδ regulates glucose metabolism and insulin sensitivity. Proc Natl Acad Sci USA 103:3444–3449
10. **Oliver Jr WR, Shenk JL, Snaith MR, Russell CS, Plunket KD, Bodkin NL, Lewis MC, Winegar DA, Sznaidman ML, Lambert MH, Xu HE, Sternbach DD, Kliewer SA, Hansen BC, Willson TM** 2001 A selective peroxisome proliferator-activated receptor δ agonist promotes reverse cholesterol transport. Proc Natl Acad Sci USA 98: 5306–5311
11. **Akiyama TE, Lambert G, Nicol CJ, Matsusue K, Peters JM, Brewer Jr HB, Gonzalez FJ** 2004 Peroxisome proliferator-activated receptor β/δ regulates very low density lipoprotein production and catabolism in mice on a Western diet. J Biol Chem 279:20874–20881
12. **Lewis GF** 1997 Fatty acid regulation of very low density lipoprotein production. Curr Opin Lipidol 8:146–153
13. **Zhang BB, Zhou G, Li C** 2009 AMPK: an emerging drug target for diabetes and the metabolic syndrome. Cell Metab 9:407–416
14. **Krämer DK, Al-Khalili L, Guigas B, Leng Y, Garcia-Roves PM, Krook A** 2007 Role of AMP kinase and PPARδ in the regulation of lipid and glucose metabolism in human skeletal muscle. J Biol Chem 282:19313–19320
15. **Bou Khalil M, Sundaram M, Zhang HY, Links PH, Raven JF, Manmontri B, Sariahmetoglu M, Tran K, Reue K, Brindley DN, Yao Z** 2009 The level and compartmentalization of phosphatidate phosphatase-1 (lipin-1) control the assembly and secretion of hepatic VLDL. J Lipid Res 50:47–58
16. **Finck BN, Gropler MC, Chen Z, Leone TC, Croce MA, Harris TE, Lawrence Jr JC, Kelly DP** 2006 Lipin 1 is an inducible amplifier of the hepatic PGC-1α/PPARα regulatory pathway. Cell Metab 4:199–210
17. **Rodríguez-Calvo R, Barroso E, Serrano L, Coll T, Sanchez RM, Merlos M, Palomer X, Laguna JC, Vázquez-Carrera M** 2009 Atorvastatin prevents carbohydrate response element binding protein activation in the fructose-fed rat by activating protein kinase A. Hepatology 49:106–115
18. **Freeman WM, Walker SJ, Vrana KE** 1999 Quantitative RT-PCR: pitfalls and potential. Biotechniques 26:112–122, 124–125
19. **Coll T, Alvarez-Guardia D, Barroso E, Gómez-Foix AM, Palomer X, Laguna JC, Vázquez-Carrera M** 2010 Activation of peroxisome proliferator-activated receptor-δ by GW501516 prevents fatty acid-induced nuclear factor-κB activation and insulin resistance in skeletal muscle cells. Endocrinology 151:1560–1569
20. **Roglans N, Verd JC, Peris C, Alegret M, Vázquez M, Adzet T, Diaz C, Hernández G, Laguna JC, Sánchez RM** 2002 High doses of atorvastatin and simvastatin induce key enzymes involved in VLDL production. Lipids 37:445–454
21. **Roglans N, Vázquez-Carrera M, Alegret M, Novell F, Zambón D, Ros E, Laguna JC, Sánchez RM** 2004 Fibrates modify the expression of key factors involved in bile-acid synthesis and biliary-lipid secretion in gallstone patients. Eur J Clin Pharmacol 59:855–861
22. **Planavila A, Alegret M, Sánchez RM, Rodríguez-Calvo R, Laguna JC, Vázquez-Carrera M** 2005 Increased Akt protein expression is associated with decreased ceramide content in skeletal muscle of troglitazone-treated mice. Biochem Pharmacol 69:1195–1204
23. **Bligh EG, Dyer WJ** 1959 A rapid method of total lipid extraction and purification. Can J Biochem Physiol 37:911–917
24. **Balgoma D, Montero O, Balboa MA, Balsinde J** 2008 Calcium-independent phospholipase A2-mediated formation of 1,2-diarachidonoyl-glycerophosphoinositol in monocytes. FEBS J 275:6180–6191
25. **Balgoma D, Astudillo AM, Pérez-Chacón G, Montero O, Balboa MA, Balsinde J** 2010 Markers of monocyte activation revealed by lipidomic profiling of arachidonic acid-containing phospholipids. J Immunol 184:3857–3865
26. **Wang YX, Zhang CL, Yu RT, Cho HK, Nelson MC, Bayuga-Ocampo CR, Ham J, Kang H, Evans RM** 2004 Regulation of muscle fiber type and running endurance by PPARδ. PLoS Biol 2:e294
27. **Wang YX, Lee CH, Tiep S, Yu RT, Ham J, Kang H, Evans RM** 2003 Peroxisome-proliferator-activated receptor δ activates fat metabolism to prevent obesity. Cell 113:159–170
28. **Higashida K, Higuchi M, Terada S** 2008 Potential role of lipin-1 in exercise-induced mitochondrial biogenesis. Biochem Biophys Res Commun 374:587–591

29. **Chakravarthy MV, Lodhi IJ, Yin L, Malapaka RR, Xu HE, Turk J, Semenkovich CF** 2009 Identification of a physiologically relevant endogenous ligand for PPARα in liver. Cell 138:476–488
30. **Sanderson LM, Boekschoten MV, Desvergne B, Müller M, Kersten S** 2010 Transcriptional profiling reveals divergent roles of PPARα and PPARβ/δ in regulation of gene expression in mouse liver. Physiol Genomics 41:42–52
31. **Zenimaru Y, Takahashi S, Takahashi M, Yamada K, Iwasaki T, Hattori H, Imagawa M, Ueno M, Suzuki J, Miyamori I** 2008 Glucose deprivation accelerates VLDL receptor-mediated TG-rich lipoprotein uptake by AMPK activation in skeletal muscle cells. Biochem Biophys Res Commun 368:716–722
32. **Gåfvels ME, Paavola LG, Boyd CO, Nolan PM, Wittmaack F, Chawla A, Lazar MA, Bucan M, Angelin BO, Strauss 3rd JF** 1994 Cloning of a complementary deoxyribonucleic acid encoding the murine homolog of the very low density lipoprotein/apolipoprotein-E receptor: expression pattern and assignment of the gene to mouse chromosome 19. Endocrinology 135:387–394
33. **Takahashi S, Kawarabayasi Y, Nakai T, Sakai J, Yamamoto T** 1992 Rabbit very low density lipoprotein receptor: a low density lipoprotein receptor-like protein with distinct ligand specificity. Proc Natl Acad Sci USA 89:9252–9256
34. **Lee WJ, Kim M, Park HS, Kim HS, Jeon MJ, Oh KS, Koh EH, Won JC, Kim MS, Oh GT, Yoon M, Lee KU, Park JY** 2006 AMPK activation increases fatty acid oxidation in skeletal muscle by activating PPARα and PGC-1. Biochem Biophys Res Commun 340:291–295
35. **Muse ED, Obici S, Bhanot S, Monia BP, McKay RA, Rajala MW, Scherer PE, Rossetti L** 2004 Role of resistin in diet-induced hepatic insulin resistance. J Clin Invest 114:232–239
36. **Du J, Guan T, Zhang H, Xia Y, Liu F, Zhang Y** 2008 Inhibitory crosstalk between ERK and AMPK in the growth and proliferation of cardiac fibroblasts. Biochem Biophys Res Commun 368:402–407
37. **Lu DY, Tang CH, Chen YH, Wei IH** 2010 Berberine suppresses neuroinflammatory responses through AMP-activated protein kinase activation in BV-2 microglia. J Cell Biochem 110:697–705
38. **Wu Y, Song P, Xu J, Zhang M, Zou MH** 2007 Activation of protein phosphatase 2A by palmitate inhibits AMP-activated protein kinase. J Biol Chem 282:9777–9788
39. **Lan F, Cacicedo JM, Ruderman N, Ido Y** 2008 SIRT1 modulation of the acetylation status, cytosolic localization, and activity of LKB1. Possible role in AMP-activated protein kinase activation. J Biol Chem 283:27628–27635
40. **Okazaki M, Iwasaki Y, Nishiyama M, Taguchi T, Tsugita M, Nakayama S, Kambayashi M, Hashimoto K, Terada Y** 2010 PPARβ/δ regulates the human SIRT1 gene transcription via Sp1. Endocr J 57:403–413
41. **Hondares E, Pineda-Torra I, Iglesias R, Staels B, Villarroya F, Giralt M** 2007 PPARδ, but not PPARα, activates PGC-1α gene transcription in muscle. Biochem Biophys Res Commun 354:1021–1027
42. **Rodríguez-Calvo R, Serrano L, Coll T, Moullan N, Sánchez RM, Merlos M, Palomer X, Laguna JC, Michalik L, Wahli W, Vázquez-Carrera M** 2008 Activation of peroxisome proliferator-activated receptor β/δ inhibits lipopolysaccharide-induced cytokine production in adipocytes by lowering nuclear factor-κB activity via extracellular signal-related kinase 1/2. Diabetes 57:2149–2157
43. **Zheng Y, Zhang W, Pendleton E, Leng S, Wu J, Chen R, Sun XJ** 2009 Improved insulin sensitivity by calorie restriction is associated with reduction of ERK and p70S6K activities in the liver of obese Zucker rats. J Endocrinol 203:337–347
44. **Ruderman NB, Xu XJ, Nelson L, Cacicedo JM, Saha AK, Lan F, Ido Y** 2010 AMPK and SIRT1: a long-standing partnership? Am J Physiol Endocrinol Metab 298:E751–E760
45. **Sugden MC, Caton PW, Holness MJ** 2010 PPAR control: it's SIRTainly as easy as PGC. J Endocrinol 204:93–104
46. **Cantó C, Gerhart-Hines Z, Feige JN, Lagouge M, Noriega L, Milne JC, Elliott PJ, Puigserver P, Auwerx J** 2009 AMPK regulates energy expenditure by modulating NAD+ metabolism and SIRT1 activity. Nature 458:1056–1060
47. **Jeninga EH, Schoonjans K, Auwerx J** 2010 Reversible acetylation of PGC-1: connecting energy sensors and effectors to guarantee metabolic flexibility. Oncogene 29:4617–4624
48. **Estall JL, Kahn M, Cooper MP, Fisher FM, Wu MK, Laznik D, Qu L, Cohen DE, Shulman GI, Spiegelman BM** 2009 Sensitivity of lipid metabolism and insulin signaling to genetic alterations in hepatic peroxisome proliferator-activated receptor-γ coactivator-1α expression. Diabetes 58:1499–1508
49. **Zhang Y, Castellani LW, Sinal CJ, Gonzalez FJ, Edwards PA** 2004 Peroxisome proliferator-activated receptor-γ coactivator 1α (PGC-1α) regulates triglyceride metabolism by activation of the nuclear receptor FXR. Genes Dev 18:157–169
50. **Chen Z, Gropler MC, Norris J, Lawrence Jr JC, Harris TE, Finck BN** 2008 Alterations in hepatic metabolism in field mice reveal a role for lipin 1 in regulating VLDL-triacylglyceride secretion. Arterioscler Thromb Vasc Biol 28:1738–1744
51. **Chakravarthy MV, Pan Z, Zhu Y, Tordjman K, Schneider JG, Coleman T, Turk J, Semenkovich CF** 2005 "New" hepatic fat activates PPARα to maintain glucose, lipid, and cholesterol homeostasis. Cell Metab 1:309–322
52. **Tanaka T, Yamamoto J, Iwasaki S, Asaba H, Hamura H, Ikeda Y, Watanabe M, Magoori K, Ioka RX, Tachibana K, Watanabe Y, Uchiyama Y, Sumi K, Iguchi H, Ito S, Doi T, Hamakubo T, Naito M, Auwerx J, Yanagisawa M, Kodama T, Sakai J** 2003 Activation of peroxisome proliferator-activated receptor δ induces fatty acid beta-oxidation in skeletal muscle and attenuates metabolic syndrome. Proc Natl Acad Sci USA 100:15924–15929